Level density and spin cutoff parameters from continuum (p, n) and (α, n) spectra*

S. M. Grimes, J. D. Anderson, J. W. McClure, B. A. Pohl, and C. Wong
Lawrence Livermore Laboratory, Livermore, California 94550

(Received 1 July 1974)

Neutron spectra produced by (p, n) reactions on ^{48}Ti, ^{49}Ti, ^{55}Mn, ^{58}Fe, and ^{63}Cu and (α, n) reactions on ^{45}Sc, ^{49}Ti, ^{51}V, ^{52}Cr, ^{58}Fe, ^{59}Co, and ^{60}Ni have been measured at four bombarding energies. The component of the spectra corresponding to equilibrium (evaporation) processes was identified from the angular and bombarding energy dependence of the continuum cross sections. Level density parameters a were deduced from the shape of the equilibrium emission spectra and spin cutoff parameters σ were obtained from the anistropy of the (α, n) angular distributions. Theoretical values for a and σ were obtained from a thermodynamic calculation with realistic single particle levels; these agreed well with the measured values. In particular, the mass number A dependence of σ was reproduced by the calculation and results from the variation with A of angular momentum values of single particle levels near the Fermi level.

[NUCLEAR REACTIONS ^{48}Ti, ^{49}Ti, ^{55}Mn, ^{58}Fe, ^{63}Cu(p, n), $E = 8-15$ MeV; ^{45}Sc, ^{49}Ti, ^{51}V, ^{52}Cr, ^{58}Fe, ^{59}Co, ^{60}Ni(α, n), $E = 12-20$ MeV; measured $\sigma(E_n, \theta)$. ^{48}V, ^{49}V, ^{52}Cr, ^{54}Mn, ^{55}Fe, ^{58}Co, ^{61}Ni, ^{62}Cu, ^{63}Zn deduced level density parameters. ^{48}V, ^{52}Cr, ^{54}Mn, ^{55}Fe, ^{61}Ni, ^{62}Cu, ^{63}Zn deduced spin cutoff parameters. Isotopically separated and natural targets.]

I. INTRODUCTION

A number of recent studies[1-12] of the reaction mechanism of proton- and α-induced reactions near $A = 60$ have yielded emission spectra for (α, α'), (α, p), (p, α) and (p, p') processes. The focus in some of these investigations has been on the role of isospin in equilibrium reactions, but in these as well as the earlier studies level density parameters for the residual nuclei reached by proton and α emission have been extracted from the data. In addition, some analyses have fitted the absolute as well as relative cross sections and have thereby inferred information about the residual nucleus reached by neutron emission.

The present experiment was undertaken to measure the neutron spectra produced in some α- and proton-induced reactions in this mass region. These measurements include some of the compound systems for which proton and α emission spectra are available and therefore provide a check on the reliability of the neutron emission channel parameters inferred from the other exit channels. Other targets corresponded to compound nuclei which could not be reached by both proton and α bombardment; these were included to investigate the systematics of level density parameters for as many residual nuclei in this mass range as possible. The reactions studied were the (α, n) reaction on ^{45}Sc, ^{49}Ti, ^{51}V, ^{52}Cr, ^{58}Fe, ^{59}Co, and ^{60}Ni and the (p, n) reaction on ^{48}Ti, ^{49}Ti, ^{55}Mn, ^{58}Fe, and ^{63}Cu.

Previous studies[13-15] of the (α, n) reaction in this mass region have shown that the statistical portion of the spectrum has a symmetric but not isotropic angular distribution. In the present experiment data were obtained at nine angles and the anisotropy of the emitted neutrons was studied as a function of both α and neutron energy. Analysis of these anistropies yielded values for the spin cutoff parameter σ. Level density parameters cannot be obtained from resonance counting at the neutron binding energy unless the value of σ is known, since these measurements give directly the density of levels of only a limited number of spins and parities. Because of a lack of experimental data, many level density compilations[16-19] have been based on calculated values for σ and an experimental check of these values is desirable.

In addition, the extraction of statistical parameters quite clearly requires that nonequilibrium contributions to the spectrum be subtracted out before a statistical analysis is attempted. Data at a number of bombarding energies were included in the present study in order to obtain information on the limits of applicability of the statistical model. Such a survey yields knowledge about the nonequilibrium component as well, but a discussion of the shape and magnitude of this portion of the spectra will be presented in a subsequent paper.

II. EXPERIMENTAL PROCEDURE

Beams of protons between 8 and 15 MeV and α particles between 11.5 and 20.4 MeV were obtained from the Livermore 2.3 m cyclotron. Neutron spectra were measured at 9 angles at 15° intervals from 15 to 135° with experimental techniques described previously.[20,21] Time-of-flight spectrometry with a 10.8 m flight path was used to determine the energy distribution of the neutrons. Scintillators (NE 213) with pulse-shape discrimination properties served as neutron detectors. Over most of the bombarding energy range a linear bias was set at a level which eliminated pulses produced by protons with energies less than 1.6 MeV; at the highest α bombarding energies, this level was raised to 3.5 MeV.

III. ANALYSES

A. Level density parameters

Experimental time-of-flight spectra were first converted to center-of-mass neutron cross sections. These were compared with calculated values for a given set of level density parameters, which were then varied until the experimental spectrum was reasonably well matched by the calculation.

Douglas and McDonald[22] have obtained the following expression for the cross section for a reaction proceeding through a compound nucleus:

$$\frac{d^2\sigma_{ab}(\epsilon_b)}{d\epsilon\, d\Omega} = \sum_{\substack{L=0 \\ \text{even}}}^{\infty} B_L(\epsilon_b) P_L(\cos\theta), \tag{1}$$

where

$$B_L(\epsilon_b) = \tfrac{1}{4}[(2I_a+1)(2i_a+1)K_a^2]^{-1} \sum_{S_a S_b I_b i_a i_b J} [G(J)]^{-1}(-1)^{S_a - S_b} T^a_{l_a}(\epsilon_a) T^b_{l_b}(\epsilon_b) Z(l_a J l_a J; S_a L) Z(l_b J l_b J; S_b L)\, \rho(U_b I_b) \tag{2}$$

and

$$G(J) = \sum_{b'} \int_0^{U_{b'}^{\max}} dU'_b \sum_{I_{b'}=0}^{\infty} T^{b'}_{l_{b'}}(\epsilon_{b'}) \sum_{S_{b'}=|J-I_{b'}|}^{J+I_{b'}} \sum_{I_{b'}=|S_{b'}-i_{b'}|}^{S_{b'}+i_{b'}} \rho_{b'}(U_{b'}, I_{b'}). \tag{3}$$

In these expressions the subscripts a and b denote entrance and exit channels, respectively, while ϵ is the channel energy, K the channel wave number, $I_a(I_b)$ the spin of target (residual) nucleus, i_a (i_b) the spin of the projectile (emitted particle), $P_L(\cos\theta)$ the Legendre polynomial of order L, S_a (S_b) is the channel spin in the entrance (exit) channel, and J is the angular momentum of the compound state. Further, l_a (l_b) denotes the orbital angular momentum in the entrance (exit) channel, $T^a_{l_a}(\epsilon_a)$ is the transmission coefficient in channel a at an energy ϵ_a for an orbital angular momentum l_a, $\rho(U_b, I_b)$ is the density of levels of spin I_b at an energy U_b in the residual nucleus corresponding to emission of particle b and $Z(l_a J l_a J; S_a L)$ and $Z(l_b J l_b J; S_b L)$ are the so-called Z coefficients, which are defined as products of Racah and Clebsch-Gordan coefficients.

This form of the Douglas and McDonald formula has been presented and discussed extensively in Refs. 6 and 9 and has been used in analyzing the data from a number of continuum spectra studied[6,7,9] in this mass region.

Initial values for the level density parameters were obtained from fits of the standard Fermi gas form to numerical values of the level density resulting from a microscopic thermodynamic calculation. Such calculations have been carried out by Sano and Yamasaki[23] and by Moretto[24] for a nucleus which is described in terms of a BCS Hamiltonian

$$H = e_k(a_k^\dagger a_k + a_{-k}^\dagger a_{-k}) - G \sum_{kk'} a_{k'}^\dagger a_{-k'}^\dagger a_k a_{-k},$$

where e_k is the energy of the kth doubly degenerate energy level, and $a_{\pm k}^\dagger$ and $a_{\pm k}$ are the creation and annihilation operators for particles with opposite spin projections. The grand partition function e^Ω of such a system can be defined as

$$\Omega = -\beta \sum_k (e_k - \lambda - E_k) + 2 \sum_k \ln[1 + \exp(-\beta E_k)] - \beta\Delta^2/G, \tag{4}$$

where Δ is the energy gap

$$E_k = [(e_k - \lambda)^2 + \Delta^2]^{1/2},$$

β is the reciprocal of the temperature, and $\lambda = \alpha/\beta$ is the chemical potential of the system. In addition, the following relation must be satisfied:

$$\frac{2}{G} = \sum_k \frac{\tanh(\frac{1}{2}\beta E_k)}{E_k}. \tag{5}$$

Values of G were determined separately for protons and neutrons so as to make Δ at zero energy equal to the pairing energies of Gilbert and Cameron.[14]

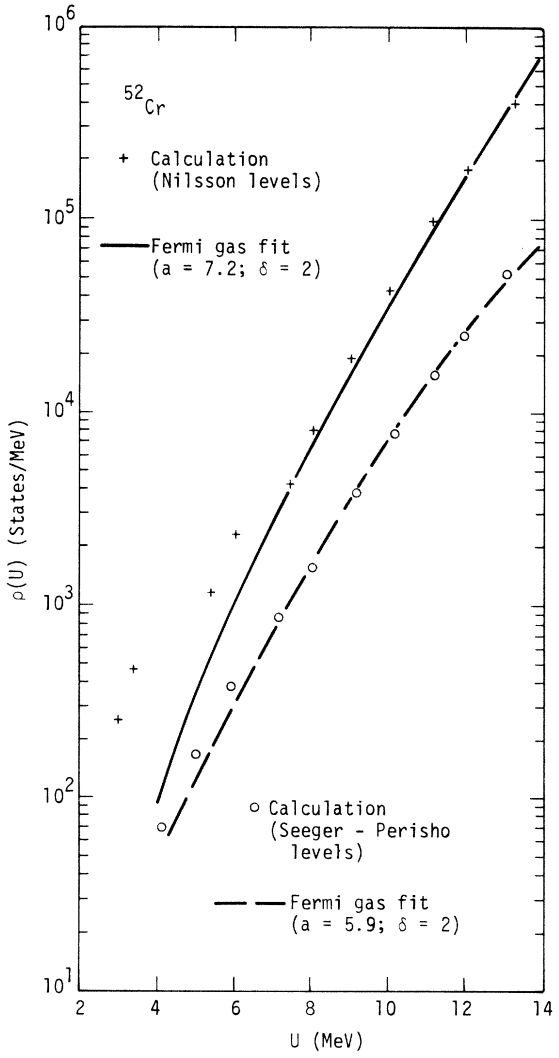

FIG. 1. Calculated state densities for ^{52}Cr. The values marked + are obtained with Nilsson single particle levels, while those marked × resulted from the use of Seeger-Perisho levels. In each case the line denotes the best-fit Fermi gas form.

TABLE I. Calculated level density parameters.

Nucleus	Seeger-Perisho a	Seeger-Perisho δ	Nilsson a	Nilsson δ
^{48}V	5.85	−2.5	6.1	−2
^{49}V	5.8	0	6.5	0
^{52}Cr	5.95	2	7.4	2
^{54}Mn	6.1	0	8.1	−1
^{55}Fe	6.2	1	8.0	1.5
^{58}Co	6.7	0	8.65	0
^{61}Ni	7.6	1.5	9.5	0.5
^{62}Cu	8.1	0	9.5	0
^{63}Zn	8.1	0.5	9.7	0.5

The state density is then

$$\rho(E,N,Z)=\left(\frac{1}{2\pi i}\right)^3 \oint d\beta \oint d\alpha_N \oint d\alpha_Z e^S ,$$

where

$$S=\Omega_N+\Omega_Z-\alpha_N N-\alpha_Z Z+\beta E . \tag{6}$$

If this integral is evaluated with the saddle-point technique, the state density is found to be

$$\rho(E)=\frac{e^S}{(2\pi)^{3/2}D^{1/2}} ,$$

where

$$D=\begin{vmatrix} \frac{\partial^2\Omega}{\partial\alpha_N^2} & \frac{\partial^2\Omega}{\partial\alpha_N\partial\alpha_Z} & \frac{\partial^2\Omega}{\partial\alpha_N\partial\beta} \\ \frac{\partial^2\Omega}{\partial\alpha_N\partial\alpha_Z} & \frac{\partial^2\Omega}{\partial\alpha_Z^2} & \frac{\partial^2\Omega}{\partial\alpha_Z\partial\beta} \\ \frac{\partial^2\Omega}{\partial\alpha_N\partial\beta} & \frac{\partial^2\Omega}{\partial\alpha_Z\partial\beta} & \frac{\partial^2\Omega}{\partial\beta^2} \end{vmatrix} . \tag{7}$$

These derivatives are obtained by differentiating Eq. (4) with respect to the appropriate variables; the explicit forms resulting from this procedure are listed by Moretto.[24] The spin cutoff parameter

TABLE II. Best-fit level density parameters.

Compound nucleus	Residual nuclei reached by emission of: Neutron	a	δ	Proton	a	δ	α	a	δ
^{49}V	^{48}V	5.8	−1.7	^{48}Ti	5.8	1.8	^{45}Sc	5.7	0
^{50}V	^{49}V	5.8	0	^{49}Ti	5.9	1.0	^{46}Sc	5.7	−1.0
^{53}Cr	^{52}Cr	6.0	2.0	^{52}Mn	6.0	−1.0	^{49}Ti	5.9	1.0
^{55}Mn	^{54}Mn	6.1	0	^{54}Cr	6.3	1.0	^{51}V	5.9	0.5
^{56}Fe	^{55}Fe	6.3	1.0	^{55}Mn	6.3	0	^{52}Cr	6.0	2.0
^{59}Co	^{58}Co	7.4	0	^{58}Fe	7.3	1	^{55}Mn	6.3	0
^{62}Ni	^{61}Ni	8.0	1.5	^{61}Co	8.0	0.5	^{58}Fe	7.3	1.0
^{63}Cu	^{62}Cu	8.1	0	^{62}Ni	8.1	3.0	^{59}Co	7.4	1.0
^{64}Zn	^{63}Zn	8.2	0	^{63}Cu	8.2	0.5	^{60}Ni	7.5	2

σ is given by

$$\sigma^2 = \sigma_p^2 + \sigma_N^2 , \tag{8}$$

where

$$\sigma_N^2 = \frac{1}{2} \sum_k \frac{m_k^2}{\cosh^2(\frac{1}{2}\beta E_k)}$$

and m_k denotes the angular momentum projection of the kth level. Finally, the level density $\rho(E, J)$ is related to $\rho(E)$ and σ as follows:

$$\rho(E, J) = \frac{(2J+1)}{2(2\pi)^{1/2}\sigma^3} \rho(E) \exp\left[-\frac{J(J+1)}{2\sigma^2}\right]. \tag{9}$$

The ground state energy is obtained by solving for the energy $(-\partial\Omega/\partial\beta)$ at zero temperature. The temperature is then incremented and the system of equations solved to determine Δ, λ, E, and $\rho(E)$ at the new temperature. This procedure is then repeated until the energy is raised outside the region of interest. As the energy increases, the pairing gap decreases, until at some point it disappears altogether, leaving the nucleus in the normal rather than the superconducting state.

To investigate the sensitivity of the calculation to the assumed single particle energies, level densities were calculated with both the single particle energies of Nilsson[25] and those of Seeger and Perisho.[26] The difference in the energy dependence

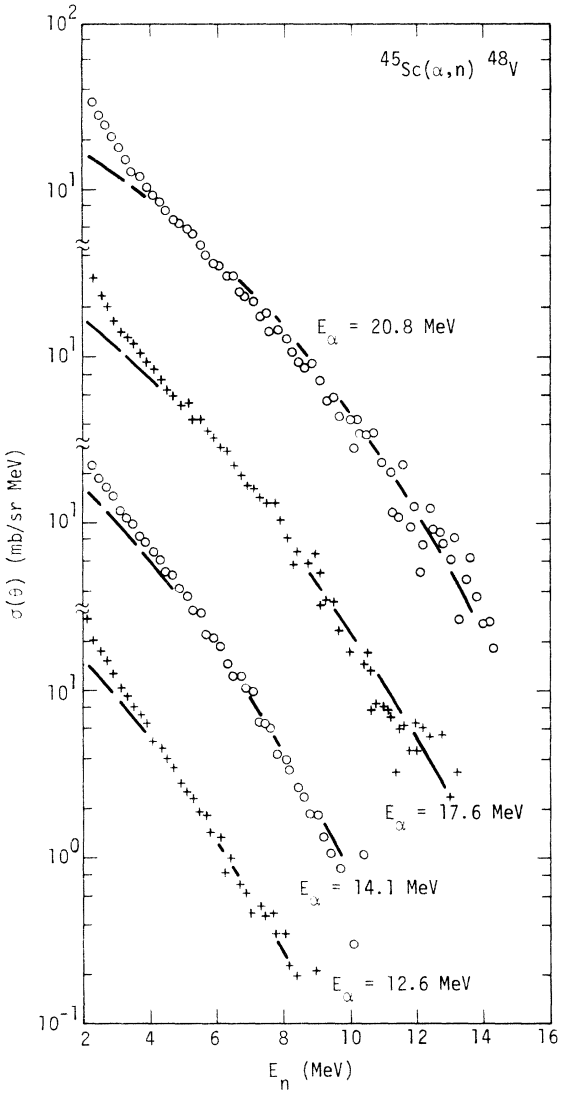

FIG. 2. The center-of-mass differential cross sections for the ^{45}Sc(α, n)^{48}V reaction at 120° for bombarding energies of 12.6, 14.1, 17.6, and 20.8 MeV. In regions where the data points were separated by 100 keV or less, an average over 200 keV has been plotted. The dashed lines indicate the cross sections calculated with the level density parameters of Table II.

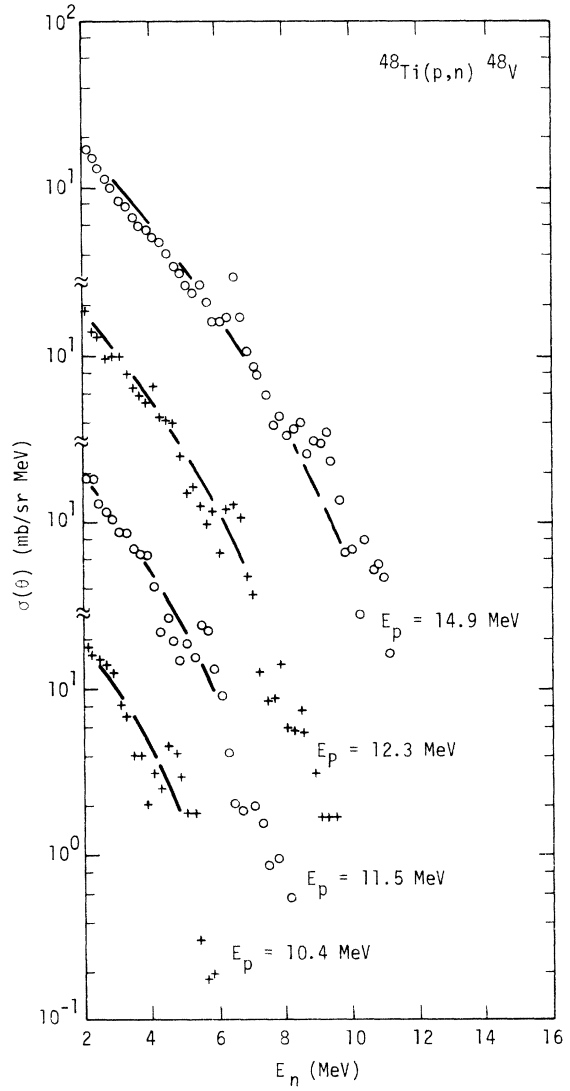

FIG. 3. The center-of-mass differential cross sections for the ^{48}Ti(p, n)^{48}V reaction. The bombarding energies were 10.4, 11.5, 12.3, and 14.9 MeV.

predicted for a given nucleus varied considerably, as can be seen in Fig. 1. The two calculations yielded very similar results for ^{48}Ti and ^{48}V, but as the nucleon number increased the values predicted by the calculation with Nilsson levels became systematically larger than the corresponding results for Seeger and Perisho levels.

Similarly, the effects of changing the pairing strengths were also investigated. Both the energy dependence of the level density below the transition point and the location of the transition point could be changed by adjusting the pairing gap, but the magnitude of the level density above the transition point was not affected by the changes in pairing strength (although the energy scale would be shifted by the change in the ground state energy).

To facilitate a comparison between experiment and the calculations, the level density values resulting from the thermodynamic calculations were fit with the Fermi gas expression in the region above the transition energy. This procedure yielded values for the level density parameter a and the energy shift δ, such that the Fermi gas expression[27]

$$\rho(U) = \frac{\sqrt{\pi}\,\exp 2[a(U-\delta)]^{1/2}}{12a^{1/4}(U-\delta)^{5/4}}$$

fit the calculated values over a 5-MeV range beyond the transition point. The values of a and δ deduced from these fits are shown in Table I.

Because the Fermi gas fit deviated from the calculated values for low excitation energies, the level density was assumed to have a constant temper-

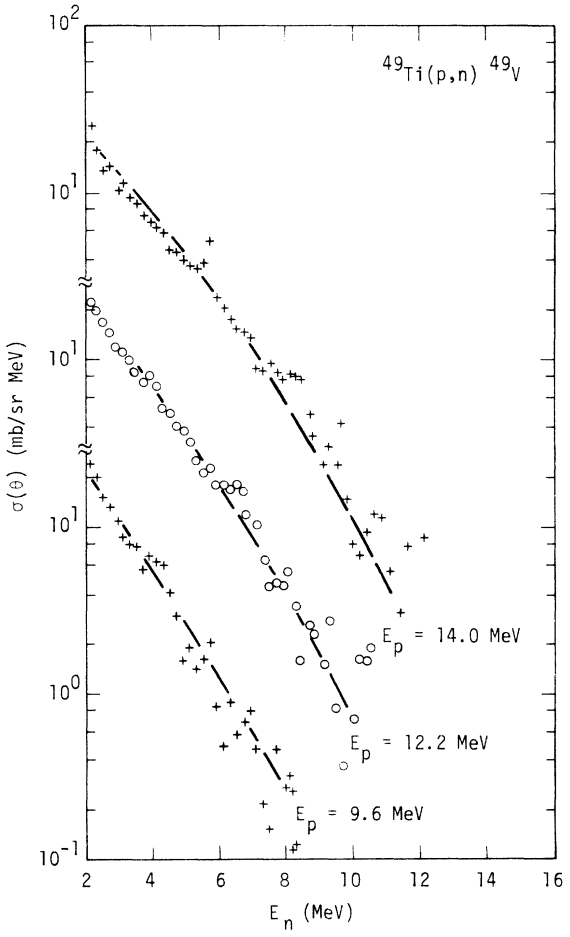

FIG. 4. The center-of-mass differential cross sections for the ^{49}Ti(p, n)^{49}V reaction. The bombarding energies were 9.6, 12.2, and 14.0 MeV.

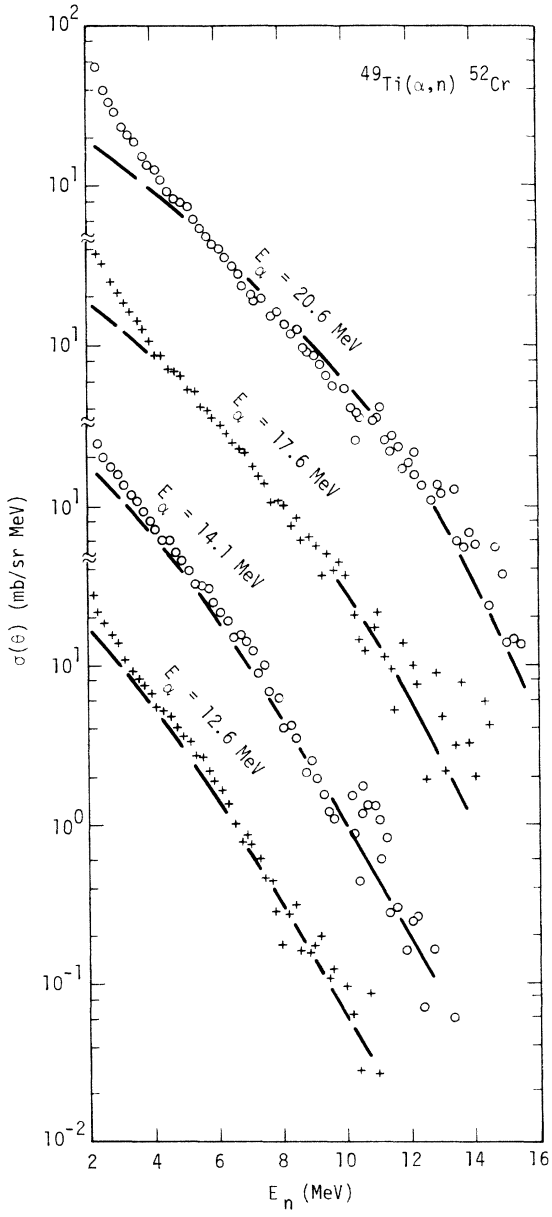

FIG. 5. The center-of-mass differential cross sections for the ^{49}Ti(α, n)^{52}Cr reaction. The bombarding energies were 12.6, 14.1, 17.6, and 20.6 MeV.

ature form below 5 MeV, with the magnitude and slope determined by continuity conditions at 5 MeV.

Since the values used in the fits were above the transition energy, changes in the pairing strength change the energy shift δ, but do not influence the level density parameter a. In contrast, the choice of single particle states has in general a large effect on a, but a much smaller influence on the energy shift.

Both sets of calculations (Seeger-Perisho and Nilsson) predict a somewhat irregular dependence of the level density parameter a on mass number A. The Nilsson calculations imply that a should increase rapidly as A changes from 48 to 52 and then more slowly between 52 and 63. In contrast, the results obtained with the use of Seeger-Perisho levels implied that a would increase slowly between A values of 48 and 54 and then more rapidly beyond $A = 54$. The a values obtained from the Nilsson calculation showed the largest change in the range of A values between 48 and 63.

Predicted values of the neutron emission cross

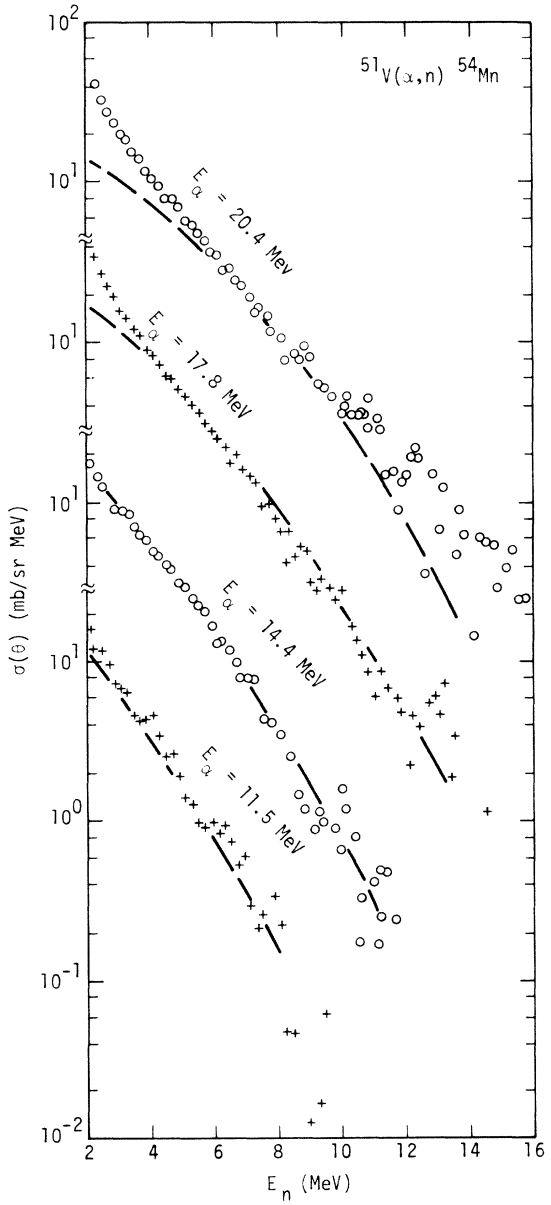

FIG. 6. The center-of-mass differential cross sections for the $^{51}V(\alpha, n)^{54}Mn$ reaction. The bombarding energies were 11.5, 14.4, 17.8, and 20.4 MeV.

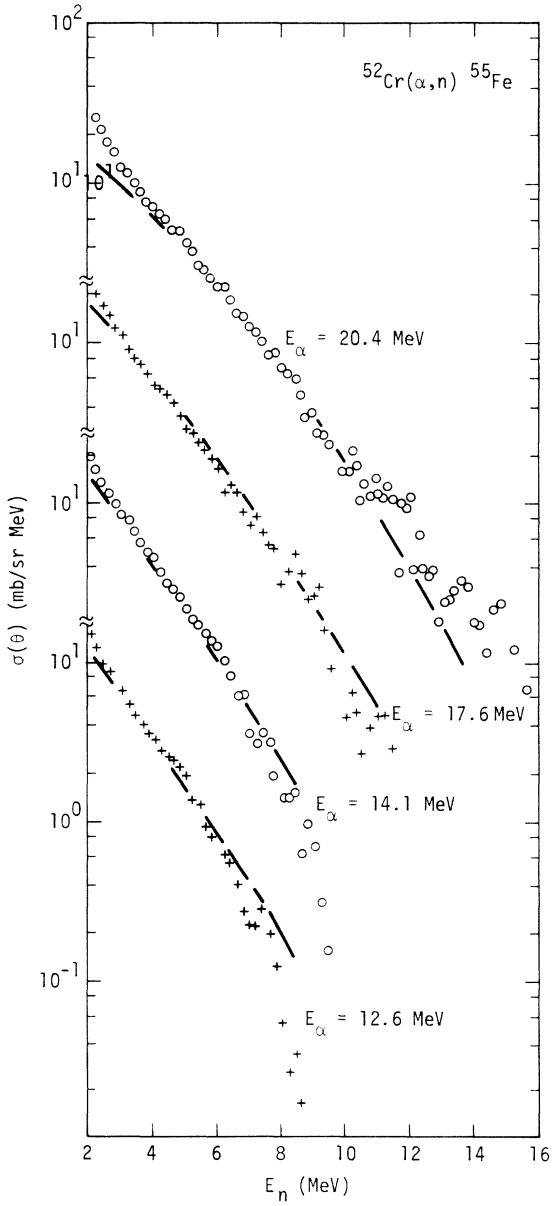

FIG. 7. The center-of-mass differential cross sections for the $^{52}Cr(\alpha, n)^{55}Fe$ reaction. The bombarding energies were 12.6, 14.1, 17.6, and 20.4 MeV.

section were obtained from Eq. (1) with the use of level density parameters resulting from the two microscopic calculations. Transmission coefficients for α particles, protons and neutrons were calculated from optical potentials suggested by Huizenga and Igo,[28] Becchetti and Greenlees,[29] and Willmore and Hodgson,[30] respectively. In general, the parameters deduced from the level density calculation with Seeger-Perisho levels yielded good fits to the experimental spectra, although in a few instances slight adjustments in the parameters were required. The resulting best fit parameters are listed in Table II. Figures 2–13 present a comparison between the experimental spectra at 120° and the calculated values corresponding to the parameters listed in Table II.

The level density parameters used for residual nuclei reached by proton and α decay are included for completeness, even though they are not directly determined by the experiment (except in cases where that same nucleus is the residual nucleus produced by neutron decay in another reaction). It is estimated that the uncertainty in the level density parameters a for nuclei reached by neutron decay is about ± 0.6; the corresponding value for the remaining nuclei is considerably larger but difficult to evaluate quantitatively, since the information about these nuclei is obtained indirectly.

It can be seen that the spectra at a number of bombarding energies are fitted by the calculations. This tests the validity of the level density parameters not only in the energy region below the neu-

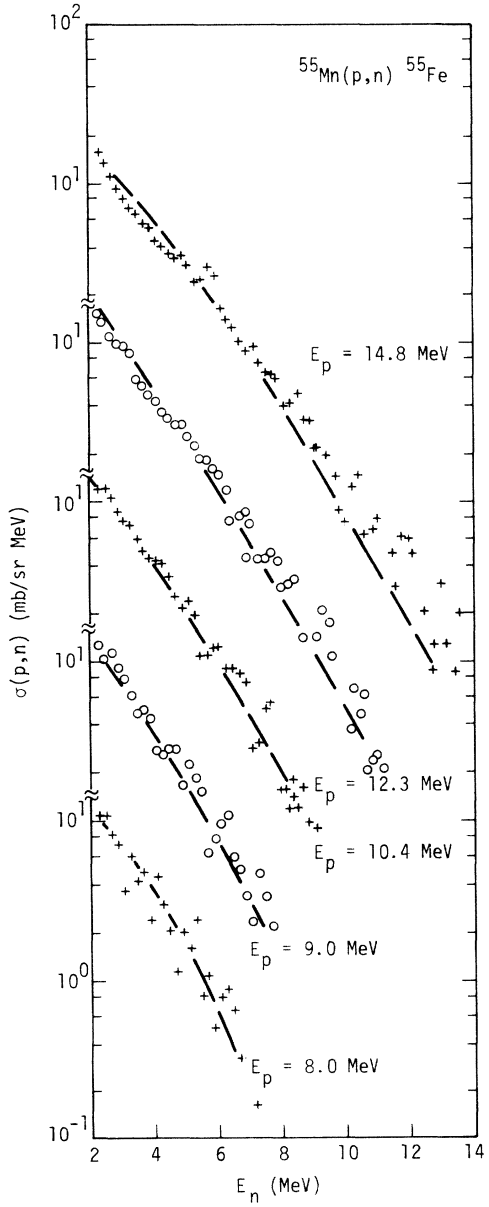

FIG. 8. The center-of-mass differential cross sections for the ^{55}Mn(p, n)^{55}Fe reaction. The bombarding energies were 8.0, 9.0, 10.4, 12.3, and 14.8 MeV.

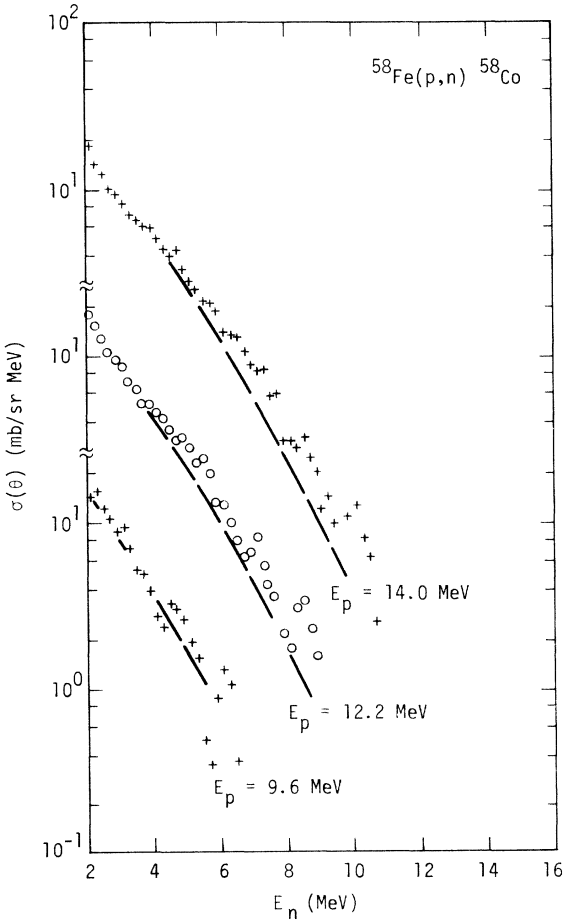

FIG. 9. The center-of-mass differential cross sections for the ^{58}Fe(p, n)^{58}Co reaction. The bombarding energies were 9.6, 12.2, and 14.0 MeV.

tron binding energy, which determine the shape of the spectra, but also the region up to the maximum residual excitation which can occur, since this (through competition) determines the magnitude of the cross section. It is not possible to use this technique to deduce level densities above about 15 MeV, because as the bombarding energy increases, the most energetic neutrons came increasingly from non-statistical reactions. As can be seen from Figs. 2–13, (p,n) and (α,n) spectra taken at bombarding energies of 15 and 20 MeV, respectively, show nonequilibrium contributions for the most energetic neutrons. At the low energy end of the spectrum for these bombarding energies, deviations between experiment and calculation occur because of the presence of second neutrons from $(p, 2n)$ and $(\alpha, 2n)$ reactions.

B. Spin cutoff parameters

The calculations described in Sec. III A yield not only the cross section as a function of energy at a given angle but also the cross section as a func-

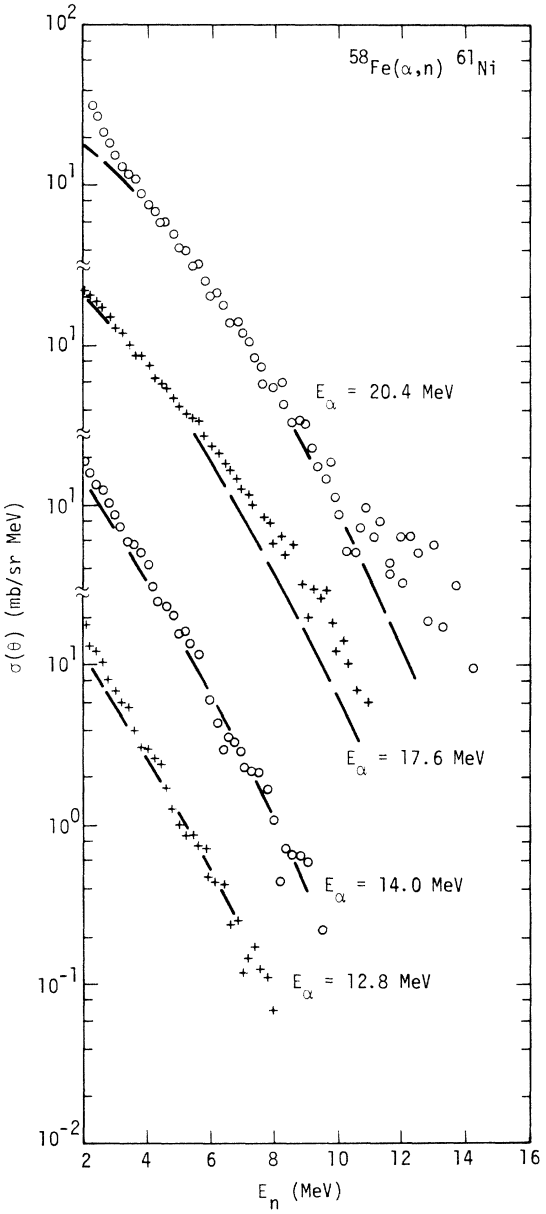

FIG. 10. The center-of-mass differential cross sections for the ^{58}Fe$(\alpha, n)^{61}$Ni reaction. The bombarding energies were 12.8, 14.0, 17.6, and 20.4 MeV.

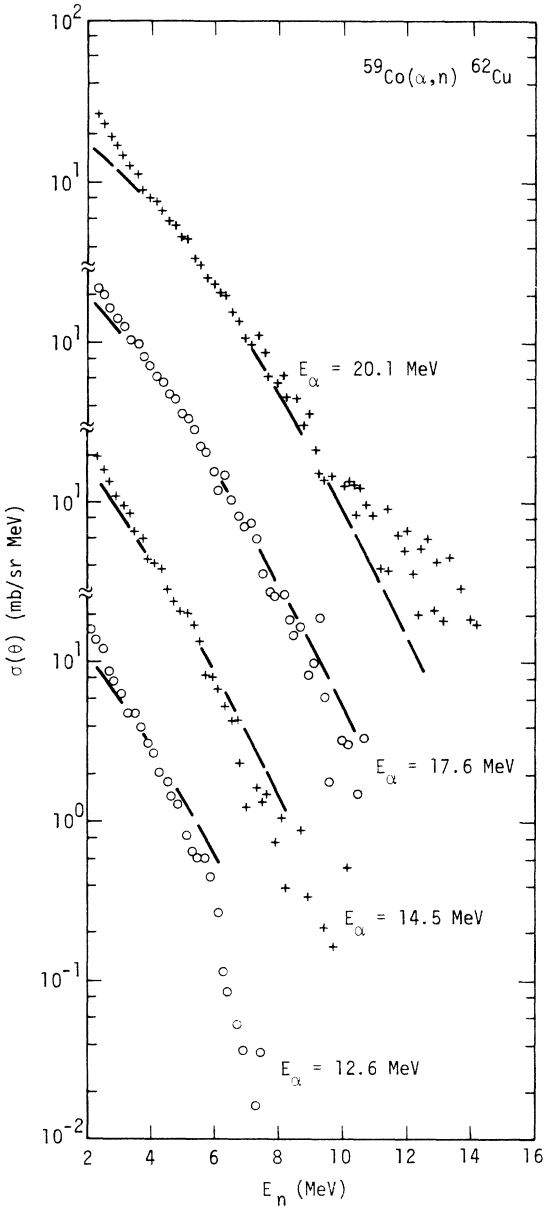

FIG. 11. The center-of-mass differential cross sections for the ^{59}Co$(\alpha, n)^{62}$Cu reaction. The bombarding energies were 12.6, 14.5, 17.6, and 20.1 MeV.

tion of angle at a given energy. As can be seen from the form of Eq. (1), the resultant angular distribution is symmetric (since only even l terms are present). The anisotropy is primarily dependent on the spin cutoff parameter σ and the average angular momentum in the entrance and exit channels, with much less sensitivity to the level density parameter a. The (p,n) spectra were characterized by anisotropies too small to be determined accurately; σ values could be inferred only from (α,n) angular distributions. Because significant parts of the 17 and 20 MeV spectra had forward-peaked angular distributions only a portion of these data could be used in determining σ values. At the lowest α bombarding energy, the (α,n) angular distributions were so slightly anistropic that most of these data were also not useful in obtaining spin cutoff parameters.

The remaining data were summed over 1-MeV intervals and the resulting angular distributions compared with values calculated from Eq. (1). Level density parameters needed for these calculations were taken from the best-fit values listed in Sec. III A. In all cases where the angular distribution was symmetric, the data could be fit with a two-term Legendre expansion. The calculations were carried out for the $l=0$, 2, and 4 terms, but at the energies of the present experiment the predicted $l=4$ term was too small to be observed.

According to Ericson[31] the Fermi gas prediction for σ is

$$\sigma^2 = It/\hbar^2, \tag{10}$$

where I is the rigid body moment of inertia ($\frac{2}{5}MR^2$) and t is the thermodynamic temperature. In turn t is related to the excitation energy and level den-

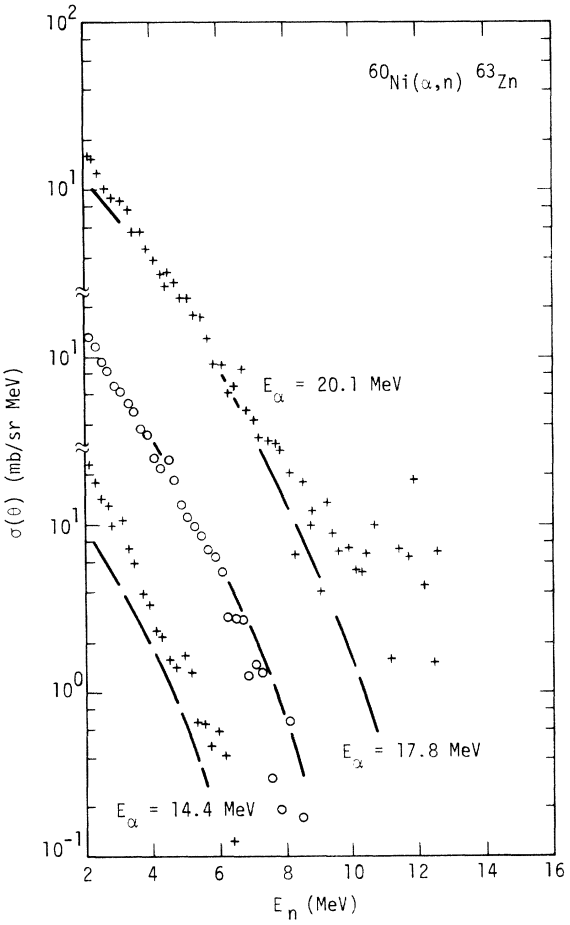

FIG. 12. The center-of-mass differential cross sections for the ^{60}Ni$(\alpha, n)^{63}$Zn reaction. The bombarding energies were 14.4, 17.8, and 20.1 MeV.

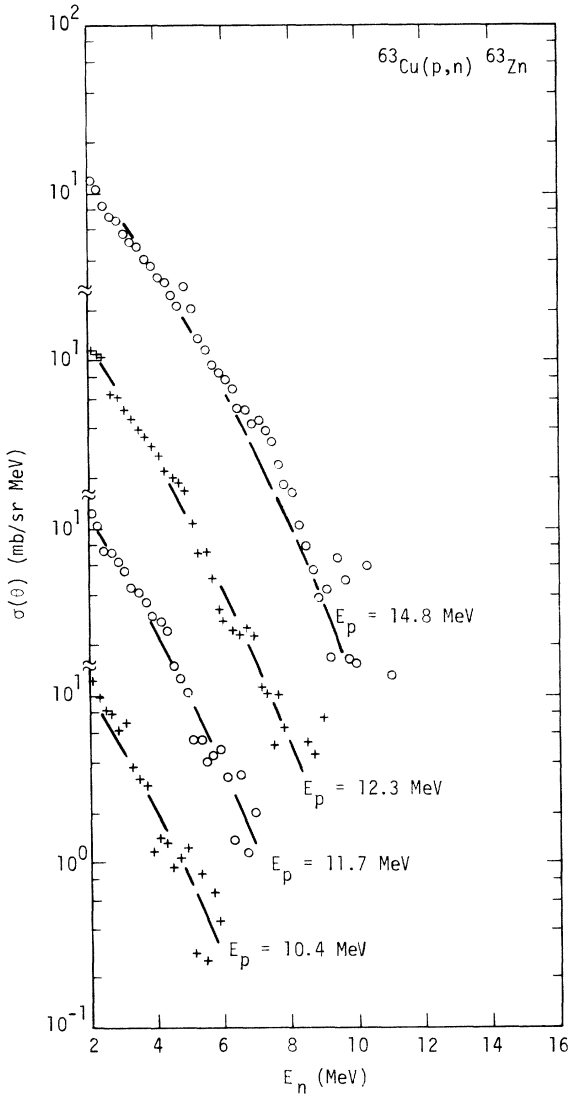

FIG. 13. The center-of-mass differential cross sections for the ^{63}Cu$(p, n)^{63}$Zn reaction. The bombarding energies are 10.4, 11.7, 12.3, and 14.8 MeV.

sity parameter a as follows:

$$t=\sqrt{U/a}\,. \tag{11}$$

Thus, if a fixed moment of inertia is assumed, σ would be expected to vary as $U^{1/4}$. Fits to the data were obtained both with a constant sigma and with an assumed $U^{1/4}$ energy dependence.

Typical anistropies expressed in terms of $\sigma(15°)/\sigma(90°)$ were about 1.25 and the individual energy-averaged cross sections were determined with a relative error of about 5%. Variations of σ^2 of 20% corresponded to changes of the calculated angular distribution which were within experimental errors. Figure 14 shows typical angular distributions and Table III presents the σ^2 values.

The values for σ^2 are those which reproduce the average anistropy for the two 1-MeV bins shown; the various values are then averaged to obtain a mean value of σ^2 for each nucleus. Finally, the calculations were repeated assuming that σ^2 varied as $U^{1/2}$ with the value at 6 MeV normalized to the mean value of σ^2 presented in Table III; this procedure also produced agreement between calculation and experiment within errors.

The most striking characteristic of the σ^2 values listed in Table III is that they apparently do not increase monotonically with A. It is generally assumed that the level density parameter a increases linearly with A; in such a case, use of Eqs. (10) and (11) predicts an A dependence of $A^{7/6}$ for σ^2. Over the range of the present measurements, this dependence would produce changes of about 35% in σ^2 between $A=48$ and 63, while the data show almost no change in the corresponding region.

The probable explanation for this discrepancy is that the angular momentum values of the single particle states nearest the Fermi level play an important role in determining σ^2. For ^{48}V, the $f_{7/2}$ orbital is partly filled for both protons and neutrons; thus, low-lying excitations will be composed primarily of particles and holes of relatively large angular momentum. Beyond ^{52}Cr, the neutrons begin filling the $p_{3/2}$ and $f_{5/2}$ orbitals, both of which are characterized by smaller angular momentum values. For Ni, Cu, and Zn, the protons have also filled the $f_{7/2}$ sub-shell, resulting in smaller angular momentum values for the proton

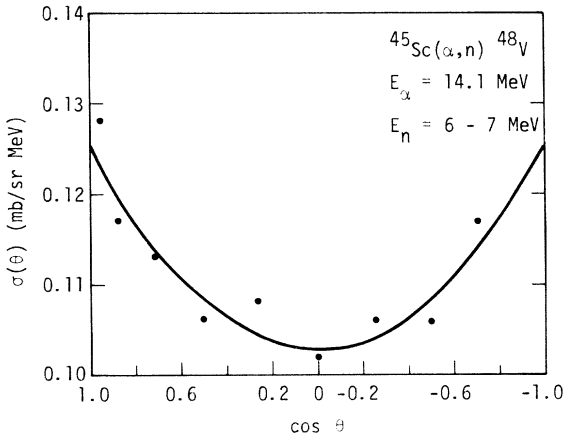

FIG. 14. Comparison of calculated and measured angular distribution for the ^{45}Sc$(\alpha, n)^{48}$V reaction at a bombarding energy of 14.1 MeV. The dots denote the measured cross section for production of neutrons with energies between 6 and 7 MeV; the line represents the calculated angular distribution for neutrons in this energy range for a σ^2 value of 14.5. The calculated values have been lowered by 6% to better illustrate the agreement in shape for this value of σ^2.

TABLE III. Measured σ^2 values.

Nucleus	Bombarding energy (MeV)	Residual excitation (MeV)	σ^2	σ^2
^{48}V	14.1	3–5	12.2	
		5–7	14.5	13.5
	17.6	5–7	13.4	
		7–9	14.4	
^{51}Cr [a]	14.0	3–5	11.3	
	14.7	3–5	12.1	
	16.0	5–7	10.8	12.3
		7–9	14.2	
	17.7	7–9	12.6	
^{52}Cr	14.1	6–8	11.1	
		8–10	12.8	12.3
	17.6	8–10	13.7	
^{54}Mn	14.4	3–5	12.1	
		5–7	12.7	12.4
	17.8	5–7	11.6	
		7–9	13.0	
^{55}Fe	14.1	3–5	12.0	
		5–7	11.5	11.9
	17.6	5–7	11.0	
		7–9	12.5	
^{59}Ni [a]	14.0	3–5	10.1	
	14.7	3–5	9.3	
	16.0	3–5	9.5	10.3
		5–7	9.8	
	17.7	5–7	10.3	
		7–9	11.3	
^{61}Ni	14.0	3–5	9.3	
		5–7	10.4	10.4
	18.2	7–9	11.6	
^{62}Cu	14.0	3–5	10.2	
	17.6	5–7	11.3	11.2
		7–9	13.1	
^{63}Zn	17.8	3–5	12.1	12.6
		5–7	13.2	

[a] From data of Ref. 15.

particles and holes as well.

Support for this interpretation is obtained from the results of the level density calculations described in Sec. III A. Equation (8) expresses the spin cutoff parameter as a sum of contributions from neutron and proton excitations, separately; the resultant σ values for the Nilsson and Seeger-Perisho single particle energies are shown in Table IV. As was the case for the level densities, the calculated values for the two single particle sets differ appreciably; better agreement with the data is obtained with the Seeger-Perisho than with the Nilsson levels. The consistency between calculation and measurement is much better for the average value of σ^2 over the range $3 \leq U \leq 9$ MeV than for the energy dependence. In general the energy dependence predicted by the thermodynamic calculation is more rapid than that predicted by the standard Fermi gas. The energy dependence of the thermodynamic calculation is in good agreement with similar calculations by Lu, Vaz, and Huizenga[32] and Behkami and Huizenga[33] for other nuclei in this mass region.

As mentioned previously, the microscopic calculations show significant shell effects. For ^{48}V, the calculated neutron and proton contributions to σ^2 are about equal, while for ^{55}Fe, the contribution at 5 MeV of protons to σ^2 is about 2.5 times that of neutrons. As A increases further, the relative proton contribution diminishes, until for ^{63}Zn at 6 MeV the two contributions are equal to within 20%. A considerably more detailed discussion of the dependence of σ values on the single particle states near the Fermi level is contained in Refs. 32 and 33.

TABLE IV. Calculated σ^2 values.

Nucleus	Seeger-Perisho levels Excitation energy (MeV)	σ^2	Nilsson levels Excitation energy (MeV)	σ^2
^{48}V	4.0	14.0	4.4	20.7
	6.0	20.8	6.0	21.2
	8.05	21.6	8.0	22.1
^{52}Cr	4.1	12.0	3.4	15.0
	6.1	14.5	6.0	16.7
	7.9	15.2	8.1	17.9
^{54}Mn	4.0	12.9	4.7	14.7
	6.0	14.8	6.05	15.7
	8.0	16.6	7.9	18.0
^{55}Fe	4.2	10.4	3.6	13.5
	6.0	12.3	6.3	14.9
	7.9	14.2	8.0	17.2
^{61}Ni	4.2	9.05	4.5	11.1
	5.6	11.5	5.95	11.6
	8.1	14.3	8.15	15.0
^{62}Cu	4.3	10.2	4.8	10.6
	6.0	13.0	6.1	12.7
	8.15	16.2	8.1	16.0
^{63}Zn	3.6	11.7	4.4	8.8
	5.95	12.3	6.1	10.8
	8.0	15.6	8.05	14.1

IV. DISCUSSION

Comparison of the present data with previous results is complicated by the fact that different level density forms[27] are used by different authors and by the interdependence of a and δ.

As has been discussed in detail by Lu, Vaz, and Huizenga,[9] the two parameters a and δ are coupled; i.e., within limits a change in one of the two may be compensated by an appropriate modification of the other to yield essentially the same absolute level density over a limited range in excitation energy. For the a and δ values in this mass region, $d\delta/da$ is positive and approximately 1. Thus, a change in a of 1 MeV^{-1} may be balanced by a corresponding change of about 1 MeV in δ.

Level density parameters predicted by Refs. 16, 17 and 19 are presented in Table V for the nuclei for which parameters were obtained in the present experiment. The values from these three compilations are in reasonable agreement in this mass region. For all nuclei except ^{54}Mn and ^{55}Fe, the a value proposed by Dilg *et al.*[19] is smaller than those of the other two compilations; the fact that the δ values of Ref. 19 are also smaller compensates to a large extent for the smaller a values.

Comparison of the level density values predicted by these parameters indicates that the level density will be smallest for the parameters of Gilbert and Cameron (GC), and larger for the parameters of Dilg *et al.* (D) and Gadioli and Zetta (GZ). The D and GZ values are very similar for A near 50, but

TABLE V. Level density parameters from compilations.

Nucleus	Gilbert and Cameron a	Gilbert and Cameron δ	Gadioli and Zetta a	Gadioli and Zetta δ	Dilg *et al.* a	Dilg *et al.* δ
^{48}V	6.8	0	6.1	−1.45	5.6	−2.1
^{49}V	6.8	1.44	6.2	0	5.7	−0.78
^{52}Cr	6.2	2.65	6.6	+1.31	5.95	+1.05
^{54}Mn	6.22	0	6.85	−1.29	6.05	−1.86
^{55}Fe	5.9	1.54	7.0	+0.27	6.1	−0.53
^{58}Co	6.5	0	7.35	−1.21	6.3	−1.74
^{61}Ni	7.02	1.2	7.75	+0.05	6.5	−0.49
^{62}Cu	7.2	0	7.85	−1.13	6.6	−1.63
^{63}Zn	7.4	1.06	8.0	−0.05	6.65	−0.45

TABLE VI. Level density parameters from other measurements.

Nucleus	a	δ	Ref.	a	δ	Ref.
^{52}Cr	7.5	2.65	10			
^{53}Mn	7.0	1.30	10			
^{55}Mn	6.8	1.27	10			
^{56}Fe [a]	6.5	2.81	10	8.5	2.81	10
^{56}Fe	6.75	2.81	8	5.7	0.7	9
^{58}Ni	7.0	2.47	10			
^{59}Co	6.63	−1	6	7.5	1.29	8
^{59}Co	6.2	−0.8	9	7.5	1.29	10
^{60}Ni	6.4	1.3	7	8.2	3.0	11,12
^{60}Ni	6.4	1.3	9			
^{61}Cu	9.0	1.29	10			
^{62}Ni	6.7	0	6	6.0	1.0	7
^{62}Ni	7.59	2.61	8			
^{62}Ni [a]	6.4	0.5	9	6.4	1.3	9
^{62}Ni	9.0	3.85	12	7.0	2.8	11
^{63}Cu	6.8	−0.5	7,9	8.9	1.41	10
^{63}Cu	8.2	1.55	12	8.3	1.55	11
^{64}Zn	8.0	2.47	10			

[a] Two sets of parameters were reported for these nuclei in one paper, based on the fits to separate reactions populating these nuclei.

the GZ values are larger for nuclei with A above 58.

The experimental values are typically between the extreme predictions of the compilations. For ^{48}V, the experimental values are close to those of D and GZ. As A increases, the experimental parameters tend to the GC values for ^{52}Cr, ^{54}Mn, and ^{55}Fe and then approach those of GZ for the largest A values. Only for ^{63}Zn is the experimental level density outside the extreme values of the compilations, and in this case the agreement with GZ parameters is within errors.

Table VI presents a summary of the level density parameters obtained in a number of similar studies utilizing charged particles.[6-12] In these experiments, the parameters were deduced from fits to emission spectra using an angular-momentum-dependent analysis similar to that used in the present paper. The values listed in Table VI are those determined directly in these experiments, i.e., those corresponding to residual nuclei in reaction channels actually measured. These values are presumably more accurate than those inferred indirectly for channels which were not observed.

The only nucleus listed in Table VI for which parameters were measured directly in the present experiment is ^{52}Cr. Reference 10 lists values for a and δ of 7.5 and 2.65, respectively, for this nucleus. These parameters yield a level density which is higher than that for the present parameters, but the difference is within errors.

The remaining nuclei listed in Table VI were not studied directly in the present experiment but may be compared with the parameters used in the calculation for nuclei reached in proton and α decay channels (because these parameters were based on the same microscopic calculations as the neutron channel nuclei, they show the same systematics as the latter parameters). For ^{55}Mn, the parameters of Sprinzak *et al.*[10] are in agreement within errors with the parameters listed in Table II. The four determinations of a and δ for ^{59}Co produce level density values which are both slightly higher[6,9] and slightly lower[8,10] than those of the present experiment; within the experimental errors, all five sets of parameters are consistent. The three sets of parameters[7,11,12] for ^{60}Ni are in good agreement with the parameters listed in Table II, with the variations in a being compensated by the differences in δ. For ^{62}Ni the parameters of Ref. 6 produce a somewhat higher, and those of Ref. 11 a somewhat lower, level density than the parameters of Refs. 7, 8, 9, and 12; the agreement of the present parameters is good with the latter four sets and fair with the former two sets. Finally, the parameters of Refs. 7, 9, and 10 for ^{63}Cu agree very well with the present values for this nucleus; the level density predicted by the parameters of Refs. 11 and 12 is slightly smaller but still agrees within errors with the present parameters.

Thus, comparison of the present results with level density obtained both from compilations and from a number of similar studies shows reasonably good agreement. The systematics of these latter parameters also support the conclusion suggested by the present data: the microscopic calculation with the Perisho-Seeger single particle levels is in better agreement with experiment than the corresponding calculation with Nilsson single particle levels.

The measured spin cutoff parameters are less consistent with either the microscopic calculations or predicted values from compilations, although the large uncertainties make the extent of the disagreement uncertain. Gilbert and Cameron predict that σ^2 will vary over the range 7 to 9.6 in this mass range, while Gadioli and Zetta predict that the variation will be between 10.5 (^{48}V at 6 MeV) and 12.7 (^{63}Zn at 6 MeV). These latter values are approximately equal to the average measured σ^2 values, although they do not agree with the A dependence as well as the microscopic calculations do. The calculated values reproduce the relative variation with A quite well but are in slight disagreement with the observed U dependence. In view of the excellent agreement between the microscopic level density calculations and the data, the inconsistencies between the corresponding spin

cutoff parameter calculations and measurements is somewhat surprising. It is possible that the present data have some unknown systematic error which distorts the measured energy dependence, but if these discrepancies are confirmed by additional measurements, they may indicate that residual interactions (in addition to pairing) must be included in calculations in order to reproduce the excitation energy dependence of the spin cutoff parameter. French and Chang[34] have calculated level densities and spin cutoff parameters including residual interactions; their results for ^{63}Cu show that, depending on the basis employed, energy dependences for σ^2 much slower than those obtained from the noninteracting fermion calculations can result. A closely related conclusion from the same calculations is that the ratio of positive to negative parity levels can differ significantly from one (~1.4) at energies as large as 10 MeV. The consequences of such a variation are expected to be small for the analysis of the present measurements, but would more directly affect the level density values deduced from low energy neutron resonance counting. Studies of level width and spacing distributions as have recently been made from low energy proton scattering[35] may help in determining whether the calculations have accurately estimated these effects.

V. SUMMARY

Neutron emission spectra produced by proton and α bombardment of a number of targets in the $A \approx 50$ mass region have been analyzed to obtain level density and spin cutoff parameters. Comparison of these values with those predicted by a microscopic thermodynamic calculation based on the single particle levels of Seeger and Perisho showed good agreement: less consistent results were obtained with the use of the single particle levels of Nilsson. The data indicate that the angular momentum values of the specific single particle orbits nearest the Fermi level strongly influence the magnitude of the spin cutoff parameter; this behavior is consistent with the microscopic calculations.

---

*Work performed under the auspices of the U. S. Atomic Energy Commission.

[1]J. Benveniste, G. Merkel, and A. Mitchell, Phys. Rev. 141, 980 (1966).
[2]H. K. Vonach and J. R. Huizenga, Phys. Rev. 149, 844 (1966).
[3]R. R. Johnson and N. M. Hintz, Phys. Rev. 153, 1169 (1966).
[4]J. Benveniste, G. Merkel, and A. Mitchell, Phys. Rev. 174, 1357 (1968).
[5]M. J. Fluss, J. M. Miller, J. M. D'Auria, N. Dudey, B. M. Foreman, Jr., L. Kowalski, and R. C. Reedy, Phys. Rev. 187, 1449 (1969).
[6]C. C. Lu, J. R. Huizenga, C. J. Stephan, and A. J. Gorski, Nucl. Phys. A164, 225 (1971).
[7]L. C. Vaz, C. C. Lu, and J. R. Huizenga, Phys. Rev. C 5, 463 (1972).
[8]A. J. Kennedy, J. C. Pacer, A. Sprinzak, J. Wiley, and N. T. Porile, Phys. Rev. C 5, 500 (1972).
[9]C. C. Lu, L. C. Vaz, and J. R. Huizenga, Nucl. Phys. A190, 229 (1972).
[10]A. Sprinzak, A. J. Kennedy, J. C. Pacer, J. Wiley, and N. T. Porile, Nucl. Phys. A203, 280 (1973).
[11]J. Wiley, J. C. Pacer, C. R. Lux, and N. T. Porile, Nucl. Phys. A212, 1 (1973).
[12]J. C. Pacer, J. Wiley, C. R. Lux, and N. T. Porile, Nucl. Phys. A226, 413 (1974).
[13]A. Alevra, R. Dumitrescu, I. Lukas, M. T. Magda, N. Martalogu, D. Plostinaru, D. Poenaru, E. Trutia, I. Vilcov, and N. Vilcov, Nucl. Phys. 58, 108 (1964).
[14]M. T. Magda, A. Alevra, I. R. Lukas, D. Plostinaru, E. Trutia, and M. Molea, Nucl. Phys. A140, 23 (1970).
[15]S. M. Grimes, J. D. Anderson, J. W. McClure, B. A. Pohl, and C. Wong, Phys. Rev. C 3, 645 (1971).
[16]A. Gilbert and A. G. W. Cameron, Can. J. Phys. 43, 1446 (1965).
[17]E. Gadioli and L. Zetta, Phys. Rev. 167, 1016 (1968).
[18]H. Vonach and M. Hille, Nucl. Phys. A127, 289 (1969).
[19]W. Dilg, W. Schantl, H. Vonach, and M. Uhl, Nucl. Phys. A217, 269 (1973).
[20]J. D. Anderson and C. Wong, Nucl. Instrum. Methods 15, 178 (1962).
[21]B. D. Walker, J. D. Anderson, J. W. McClure, and C. Wong, Nucl. Instrum. Methods 29, 333 (1964).
[22]A. C. Douglas and N. MacDonald, Nucl. Phys. 13, 382 (1959).
[23]M. Sano and S. Yamasaki, Prog. Theor. Phys. 29, 397 (1963).
[24]L. G. Moretto, Nucl. Phys. A182, 641 (1972).
[25]S. G. Nilsson, K. Dan. Vid. Selsk. Mat.-Fys. Medd. 29, No. 16 (1955).
[26]P. A. Seeger and R. C. Perisho, Los Alamos Scientific Laboratory Report No. LA-3751 (1967).
[27]In many papers an alternative form is used in which $(U-\delta)^{5/4}$ is replaced by $(U-\delta+t)^{5/4}$. This discrepancy is due to the different procedures used in carrying out the saddle point integration. See D. W. Lang, Nucl. Phys. 26, 434 (1961) for a detailed explanation. Use of the alternative form in the fits to the calculated level density values would have left the a values essentially unaltered but would have changed the energy shifts by about 0.5 MeV (decreasing the magnitude of shifts which were greater than zero and increasing the size of shifts which are less than zero).
[28]J. R. Huizenga and G. Igo, Nucl. Phys. 29, 473 (1962).

[29]F. D. Becchetti, Jr., and G. W. Greenlees, Phys. Rev. 182, 1190 (1969).
[30]D. Willmore and P. E. Hodgson, Nucl. Phys. 55, 673 (1964).
[31]T. Ericson, Adv. Phys. 9, 425 (1960).
[32]C. C. Lu, L. C. Vaz, and J. R. Huizenga, Nucl. Phys. A197, 321 (1972).
[33]A. N. Behkami and J. R. Huizenga, Nucl. Phys. A217, 78 (1973).
[34]J. B. French and F. S. Chang, in *Statistical Properties of Nuclei*, edited by J. B. Garg (Plenum, New York, 1972), p. 405.
[35]J. D. Moses, H. W. Newson, E. G. Bilpuch, and G. E. Mitchell, Nucl. Phys. A175, 556 (1971).